



PCCP

**The luminescence properties of the heteroleptic
[Re(CO)₃(N \bar{N} N)Cl] and [Re(CO)₃(N \bar{N} N)(CH₃CN)]⁺
complexes in view of the combined Marcus-Jortner and
Mulliken-Hush formalism**

Journal:	<i>Physical Chemistry Chemical Physics</i>
Manuscript ID	CP-ART-08-2015-005167.R1
Article Type:	Paper
Date Submitted by the Author:	13-Oct-2015
Complete List of Authors:	Woźna, Agnieszka; University of Siedlce, Faculty of Sciences, Institute of Chemistry, Kapturkiewicz, Andrzej; University of Siedlce, Faculty of Sciences, Institute of Chemistry

SCHOLARONE™
Manuscripts



PCCP

PAPER

The luminescence properties of the heteroleptic $[\text{Re}(\text{CO})_3(\text{N}\cup\text{N})\text{Cl}]$ and $[\text{Re}(\text{CO})_3(\text{N}\cup\text{N})(\text{CH}_3\text{CN})]^+$ complexes in view of the combined Marcus-Jortner and Mulliken-Hush formalism

Agnieszka Woźna and Andrzej Kapturkiewicz*

The luminescence properties of the heteroleptic *fac*- $\text{Re}(\text{CO})_3^+$ complexes with α -diimine $\text{N}\cup\text{N}$ ligands, neutral $[\text{Re}(\text{CO})_3(\text{N}\cup\text{N})\text{Cl}]$ and cationic $[\text{Re}(\text{CO})_3(\text{N}\cup\text{N})(\text{CH}_3\text{CN})]^+$ species have been studied in acetonitrile solutions at room temperature. The investigated complexes exhibit the metal to ligand charge-transfer (MLCT) phosphorescence with the emission characteristics strongly affected by the nature of coordinated α -diimine $\text{N}\cup\text{N}$ ligands. The observed trends can be quantitatively described by invoking the electronic interactions between $^3\text{MLCT}$ and ^3LC states as well as the spin-orbit interactions between $^3\text{MLCT}$ and $^1\text{MLCT}$ states, respectively. All quantities necessary for the description can be straightforwardly accounted from analysis of the radiative $^1\text{MLCT} \leftarrow \text{S}_0$ and $^3\text{MLCT} \rightarrow \text{S}_0$ charge transfer processes. It is also demonstrated that the radiative k_r and non-radiative k_{nr} decay rate constants of the excited $^3\text{MLCT}$ states can be interpreted within the same set of parameters. As expected from the Mulliken-Hush formalism the both processes are strictly related that allows prediction of the non-radiative k_{nr} rate constants using the parameters available from analysis of the radiative $^1\text{MLCT} \leftarrow \text{S}_0$ and $^3\text{MLCT} \rightarrow \text{S}_0$ charge transfer processes.

Received 00th January 20xx,
Accepted 00th January 20xx

DOI: 10.1039/x0xx00000x

www.rsc.org/pccp

Introduction

Light emitting transition metal complexes with organic ligands have found prevalent interest due to their potential application in many modern optoelectronic applications. These include light-to-electricity conversion¹⁻³ (dye-sensitized solar cells – DSSC) as well as electricity-to-light conversion⁴⁻⁶ (organic light emitting devices – OLED). Other important examples are chemical and biological sensors⁷⁻⁹, photo-catalysts¹⁰⁻¹² or photodynamic therapy.¹³⁻¹⁵

Organometallic emitters are interesting species not only due to their practical applications but also from the theoretical point of view. The later interest arises from the fact that the emissive properties of these complexes are usually very different from those typical for “pure” organic molecules.^{16,17} Despite that, the photophysical properties of organic and organometallic compounds can be understood in similar manner following the same general lines usually based on the Jablonski diagram. The picture is, however, more multifaceted in the case of organometallic emitters because of presence of a panoply of the electronic excited-states for such species and strong spin-orbit coupling (SOC) between them caused by the presence of heavy metal ion(s). The SOC effects are especially important for complexes with the 4d or 5d metal ions.

The photophysical and photochemical behaviour of the transition metal complexes are governed by the relative energetic position and the interplay of the closely lying excited states of different character. In the general case, apart from the excitation localized/delocalized within individual ligand/ligands (LC) or metal ion(s) (MC), these may include metal-to-ligand charge-transfer (MLCT), ligand-to-metal charge transfer (LMCT), metal-to-metal charge transfer (MMCT), and ligand-to-ligand charge transfer (LLCT) states. Fortunately, in many cases the actual picture can be simplified considering only these of the excited states that are essential for the proper description of the observed properties of organometallic emitters.

Depending on the metal/ligand(s) combination, the photophysical and photochemical properties of organometallic emitters may be quite different even for the same metal ion with pretty similar ligands present in its coordination sphere. Typical examples are *fac*- $\text{Re}(\text{CO})_3^+$ complexes¹⁸⁻²⁴ with bidentate $\text{N}\cup\text{N}$ α -diimine ligands (e.g., 2,2'-bipyridine or 1,10-phenanthroline and their derivatives), neutral $[\text{Re}(\text{CO})_3(\text{N}\cup\text{N})\text{X}]$ (where X = anions like Cl^- , Br^- , CN^-) and ionic $[\text{Re}(\text{CO})_3(\text{N}\cup\text{N})\text{L}]^+$ (where L = monodentate ligand axial to the $\text{N}\cup\text{N}$ plane). Appropriately changing $\text{N}\cup\text{N}$ and X or L ligands attached to the *fac*- $\text{Re}(\text{CO})_3^+$ core one can precisely tune character of the observed emission from the excited $^3\text{MLCT}$ to ^3LC state with the excitation localized within $\text{N}\cup\text{N}$ or (sometimes) L ligand. The emission from *fac*- $\text{Re}(\text{CO})_3^+$ chelates is also sensitive to many other factors like temperature or medium rigidity. It makes *fac*- $\text{Re}(\text{CO})_3^+$ complexes ideal candidates for testing the relationships between the structure of the transition metal

Institute of Chemistry, Faculty of Sciences, Siedlce University of Natural Sciences and Humanities, 3 Maja 54, 08-110 Siedlce, Poland
E-mail: andrzej.kapturkiewicz@uph.edu.pl. Phone: +48-25-643-10-97.

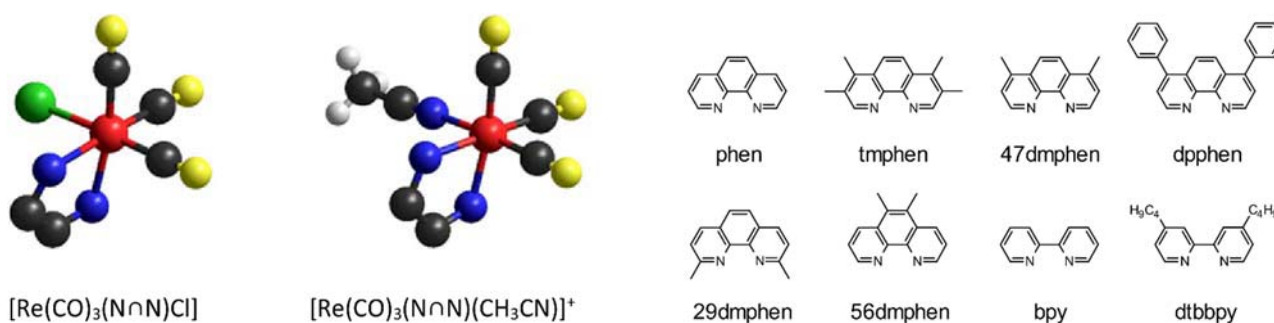


Fig. 1 Ligands orientation around the central Re^+ ion in the studied neutral $[\text{Re}(\text{CO})_3(\text{N}\cap\text{N})\text{Cl}]$ and cationic $[\text{Re}(\text{CO})_3(\text{N}\cap\text{N})(\text{CH}_3\text{CN})]^+$ complexes (left) and structures of the bidentate α -diimine $\text{N}\cap\text{N}$ ligands employed (right). Acronyms used for $\text{N}\cap\text{N}$ ligands: 1,10-phenanthroline – phen, 3,4,7,8-tetramethyl-1,10-phenanthroline – tmphen, 4,7-dimethyl-1,10-phenanthroline – dmphen, 4,7-diphenyl-1,10-phenanthroline – dpphen, 2,9-dimethyl-1,10-phenanthroline – 29dmphen, 5,6-dimethyl-1,10-phenanthroline – 56dmphen, 2,2'-bipyridine – bpy, and 4,4'-di-*t*-butyl-2,2'-bipyridine – dtbbpy.

complexes and their photophysical and photochemical properties – one of the most important tasks in inorganic physical chemistry.

The above stated, monotonic changes in the nature of organometallic emitters from the excited $^3\text{MLCT}$ to ^3LC state seems to be more or less characteristic for many other emissive organometallic derivatives, especially for complexes of $4d^6$ and $5d^6$ ions like Ru^{2+} , Os^{2+} or Ir^{3+} .^{15,16,23-25} This arises from the comparable energies of the excited ^3LC states (typically 2-3 eV for most of π -aromatic ligands) and $^3\text{MLCT}$ states emitting in the visible part of UV-vis radiation. The situation is similar to that characteristic for “pure” organic intramolecular charge-transfer states when the electronic interaction between the excited CT state $^1\text{A}^-\text{D}^+$ and locally excited states localized within the acceptor – ^1A and/or donor – ^1D subunits forming a given A–D molecule play a crucial role.^{26,27}

Both fundamental, the radiative and non-radiative deactivation $^1\text{A}^-\text{D}^+ \rightarrow \text{S}_0$ and $^3\text{MLCT} \rightarrow \text{S}_0$ processes recovering the ground state S_0 can be discussed in the terms of electron transfer in the inverted Marcus region.²⁸⁻³¹ The same is also valid for the radiative $^1\text{A}^-\text{D}^+ \leftarrow \text{S}_0$ and $^1\text{MLCT} \leftarrow \text{S}_0$ transitions. It means that the same approach can be used in description of the excited $^1\text{A}^-\text{D}^+$ and $^3\text{MLCT}$ species. Some intrinsic information on properties of the excited $^1\text{A}^-\text{D}^+$ or $^3\text{MLCT}$ states can be independently obtained from the comparative analysis of the CT and MLCT absorption band exemplifying the radiative charge separation and/or from the kinetics of the radiative and non-radiative charge recombination. All of these processes can be described using a “Golden rule” type formula leading to the appropriate rate constant that is principally dependent on two quantities, a Franck-Condon weighted density of states (function of energetic and nuclear parameters) and the electronic matrix elements (V) describing the electronic coupling between the states involved in the given transition. Relatively simple estimation of the above-mentioned factors is possible from a band-shape analysis of the CT/MLCT absorption and/or luminescence and values of transition dipole moments of the charge-transfer absorption (M_{abs}) and emission (M_{em}), correspondingly. Moreover, in the case of MLCT systems the above described methodology allows also estimation of the

spin-orbit coupling elements (V_{SOC}) describing interactions between the excited $^1\text{MLCT}$ and $^3\text{MLCT}$ states.³²

Systematic studies of connections between the related optical and thermal electron transfer, however, are not thoroughly performed. Only a limited amount of organic CT or organometallic MLCT systems have been explored to date in this way despite that the physical formalism describing the issue seems to be quite intuitive. Typically CT and MLCT luminescence properties of newly synthesized compounds are mainly analysed by means of more or less advanced quantum-mechanical calculation. Despite of its versatility such approach may lead to serious over-interpretation of the experimental spectroscopic data because the quantum-mechanical calculations (also those done with the use of TD-DFT method) usually wrongly estimate the energies of the excited charge-transfer states.^{33,34} Thus, particularly in the case when the excited $^1\text{D}/^1\text{A}$ and $^1\text{A}^-\text{D}^+$ or ^3LC and $^3\text{MLCT}$ states are close in energy, an additional information about the nature of the emissive $^1\text{A}^-\text{D}^+$ or $^3\text{MLCT}$ species may be crucial for proper interpretation of their properties.

As mentioned above the combined Mulliken-Hush (applied in the analysis of M_{abs} and M_{em} values) and Marcus-Jortner (applied in the determination of energetic and nuclear quantities associated with charge-transfer processes) formalisms are not often used in the description of CT or MLCT phenomena. One can hope, however, that such approach will become more commonly used if any other, different from those already elaborated, CT or MLCT system will be effectively analysed. To follow this anticipation we have decided to reinvestigate the photophysical properties of the famous organometallic luminophores containing *fac*- $\text{Re}(\text{CO})_3^+$ core. Although the α -diimine complexes with this ion have been widely studied (including band shape analysis of their luminescence spectra³⁵⁻³⁷) we have found that some additional information about nature of the excited $^3\text{MLCT}$ states will become available when results from the ordinary spectroscopic measurements (UV-vis absorption and emission spectra, emission quantum yields ϕ_{em} and lifetimes τ_{em}) are analysed in a somewhat more sophisticated way. As the model systems for our studies we have selected easily synthetically affordable *fac*- $\text{Re}(\text{CO})_3^+$ chelates, the neutral $[\text{Re}(\text{CO})_3(\text{N}\cap\text{N})\text{Cl}]$ and their cationic

Table 1 Spectroscopic and photophysical properties of the cationic $[\text{Re}(\text{CO})_3(\text{N}\pi\text{N})(\text{CH}_3\text{CN})]^+$ and neutral $[\text{Re}(\text{CO})_3(\text{N}\pi\text{N})\text{Cl}]$ complexes. Absorption maxima $\tilde{\nu}_{\text{abs}}^{\text{max}}$, molar extinction coefficients ϵ_{M} , and transition dipole moments M_{abs} of $^1\text{MLCT} \leftarrow \text{S}_0$ transitions. Emission maxima $\tilde{\nu}_{\text{em}}^{\text{max}}$, emission quantum yields ϕ_{em} , lifetimes τ_{em} , resulting radiative k_{r} and non-radiative k_{nr} rate constant, and transition dipole moments M_{em} of $^3\text{MLCT} \rightarrow \text{S}_0$ transitions.

Complex type	$^1\text{MLCT} \leftarrow \text{S}_0$ transition			$^3\text{MLCT} \rightarrow \text{S}_0$ transition						
	Ligand N π N	$\tilde{\nu}_{\text{abs}}^{\text{max}} / \text{cm}^{-1}$	$\epsilon_{\text{M}} / \text{M}^{-1}\text{cm}^{-1}$	$M_{\text{abs}} / \text{D}$	$\tilde{\nu}_{\text{em}}^{\text{max}} / \text{cm}^{-1}$	ϕ_{em}	$\tau_{\text{em}} / \mu\text{s}$	$k_{\text{r}} / \text{s}^{-1}$	$k_{\text{nr}} / \text{s}^{-1}$	M_{em} / D
$[\text{Re}(\text{CO})_3(\text{N}\pi\text{N})(\text{CH}_3\text{CN})]^+$										
dpphen				17420	0.45	15.7	2.9×10^4	3.5×10^4		0.077
bpy				17500	0.14	0.59	2.4×10^5	1.5×10^6		0.221
dbbpy				17900	0.20	0.71	2.8×10^5	1.1×10^6		0.233
phen				18000	0.37	3.1	1.2×10^5	2.0×10^5		0.150
29dmphen				18400	0.13	1.7	7.7×10^4	5.1×10^5		0.117
56dmphen				18400	0.40	42.4	9.4×10^3	1.4×10^4		0.041
47dmphen				19440	0.19	10.7	1.8×10^4	7.6×10^4		0.052
tmphen				19350	0.21	16.1	1.3×10^4	4.9×10^4		0.045
$[\text{Re}(\text{CO})_3(\text{N}\pi\text{N})\text{Cl}]$										
dpphen	26950	7.8×10^3	2.7	15100	0.031	0.32	9.7×10^4	3.0×10^6		0.176
bpy	26950	3.2×10^3	1.7	15400	0.006	0.048	1.3×10^5	2.1×10^7		0.194
dbbpy	27470	3.4×10^3	1.8	15650	0.015	0.089	1.7×10^5	1.1×10^7		0.220
phen	27250	3.9×10^3	1.9	15650	0.022	0.15	1.5×10^5	6.5×10^6		0.205
29dmphen	26880	1.9×10^3	1.3	15850	0.014	0.069	2.0×10^5	1.4×10^7		0.237
56dmphen	26180	4.3×10^3	2.0	15750	0.025	0.23	1.1×10^5	4.2×10^6		0.175
47dmphen	28250	4.6×10^3	2.0	16300	0.057	0.64	8.9×10^4	1.5×10^6		0.151
tmphen	~ 29000	$\sim 2.0 \times 10^3$	~ 1.3	16750	0.12	1.9	6.8×10^4	4.7×10^5		0.126

$[\text{Re}(\text{CO})_3(\text{N}\pi\text{N})(\text{CH}_3\text{CN})]^+$ analogues (cf. Fig. 1). In this communication we present the obtained results.

Results and discussion

$^1\text{MLCT} \leftarrow \text{S}_0$ absorption and $^3\text{MLCT} \rightarrow \text{S}_0$ emission

The results of the room-temperature experiments are summarized in Table 1. The measurements have been performed in acetonitrile solutions to surely exclude potentially possible replacement of the monodentate CH_3CN ligand attached to $\text{fac-Re}(\text{CO})_3^+$ core according to $[\text{Re}(\text{CO})_3(\text{N}\pi\text{N})(\text{CH}_3\text{CN})]^+ \rightarrow [\text{Re}(\text{CO})_3(\text{N}\pi\text{N})(\text{solvent})]^+$ reaction. Whereas the neutral $[\text{Re}(\text{CO})_3(\text{N}\pi\text{N})\text{Cl}]$ chelates are very stable species, their cationic $[\text{Re}(\text{CO})_3(\text{N}\pi\text{N})(\text{CH}_3\text{CN})]^+$ analogues are more labile that make them useful as starting material in preparation of other $[\text{Re}(\text{CO})_3(\text{N}\pi\text{N})\text{L}]^+$ complexes by the ligand exchange. On contrary to that, a prolonged heating of the solutions containing $[\text{Re}(\text{CO})_3(\text{N}\pi\text{N})\text{Cl}]$ and AgClO_4 (or other Ag^+ salts) is required for abstraction of Cl^- ion.

The acquired UV-vis absorption spectra (cf. Fig. 2) are very similar to those reported previously in the literature and the assignments have been made accordingly.³⁸⁻⁴² The spectral maxima of the low-energy absorption band (below ca. 30000 cm^{-1}) and the more intense higher energy absorption bands are the characteristic MLCT and $^*\pi \leftarrow \pi$ transitions, respectively. In the case of the studied neutral $[\text{Re}(\text{CO})_3(\text{N}\pi\text{N})\text{Cl}]$ chelates quite well separated $^1\text{MLCT} \leftarrow \text{S}_0$ and $^1\text{LC} \leftarrow \text{S}_0$ bands can be clearly seen. It allows quite precise determination of ϵ_{M} (molar extinction coefficient), $\tilde{\nu}_{\text{abs}}^{\text{max}}$ (position of absorption maximum), and $\Delta\tilde{\nu}_{1/2}$ (spectral width) quantities characterizing the optical $^1\text{MLCT} \leftarrow \text{S}_0$ transitions. These quantities can be

straightforwardly used in estimation of the transition dipole moment M_{abs} values. The found M_{abs} values in the range of 1.3-2.0 D are characteristic for most of the neutral $[\text{Re}(\text{CO})_3(\text{N}\pi\text{N})\text{Cl}]$ chelates studied in this work. Only in the case of $[\text{Re}(\text{CO})_3(\text{dpphen})\text{Cl}]$ complex the estimated M_{abs} value is somewhat larger being equal to 2.7 D. In the performed estimation of M_{abs} values so-called the "lazy man's" approximation⁴³ have been used because principally more correct approach based on the integrated absorption band intensity^{44,45} could not be applied due to the partial overlap of $^1\text{MLCT} \leftarrow \text{S}_0$ and $^1\text{LC} \leftarrow \text{S}_0$ bands.

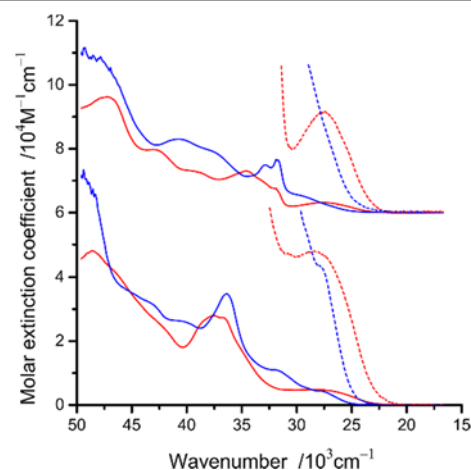


Fig. 2 UV-vis absorption spectra of the investigated neutral $[\text{Re}(\text{CO})_3(\text{N}\pi\text{N})\text{Cl}]$ (red lines) and cationic $[\text{Re}(\text{CO})_3(\text{N}\pi\text{N})(\text{CH}_3\text{CN})]^+$ (blue lines) complexes. Data for N π N = 47dmphen (bottom) and dtbbpy (top). Spectra of $[\text{Re}(\text{CO})_3(\text{dtbbpy})\text{Cl}]$ and $[\text{Re}(\text{CO})_3(\text{dtbbpy})(\text{CH}_3\text{CN})]^+$ are shifted along Y-axis by a factor 6×10^4 . Low-energy parts of the spectra are expanded by a factor 10 to emphasize low intensity $^1\text{MLCT} \leftarrow \text{S}_0$ transitions.

UV-vis absorption spectra of the studied cationic $[\text{Re}(\text{CO})_3(\text{N}\text{O}\text{N})(\text{CH}_3\text{CN})]^+$ complexes are pretty similar to those recorded for their neutral $[\text{Re}(\text{CO})_3(\text{N}\text{O}\text{N})\text{Cl}]$ counterparts. The main difference is the hypsochromic shift (*ca.* 2000 cm^{-1}) of ${}^1\text{MLCT} \leftarrow \text{S}_0$ transitions. It makes the overlap of ${}^1\text{MLCT}$ and ${}^*\pi \leftarrow \pi$ bands still more pronounced that precludes enough precise estimation of ε_{M} , $\tilde{\nu}_{\text{abs}}^{\text{max}}$, and $\Delta\tilde{\nu}_{1/2}$ quantities (for this reason not reported in Table 1). Nevertheless, one can conclude that the M_{abs} values characterizing ${}^1\text{MLCT} \leftarrow \text{S}_0$ transitions are (in the case of the same NON ligand) similar for both types of the studied *fac*- $\text{Re}(\text{CO})_3^+$ chelates.

Typical examples of the room temperature emission spectra for a number of the complexes are shown in Fig. 3. The complexes displayed broad emission spectra which can be assigned as MLCT-based luminescence, characteristic for this type of luminophores.³⁸⁻⁴² Moreover, following trends for emission energy maxima, the emission spectra show a clear progression from the broad structureless emission (low energy emitters) to slightly structured emission (high energy $[\text{Re}(\text{CO})_3(\text{tmphen})(\text{CH}_3\text{CN})]^+$ and $[\text{Re}(\text{CO})_3(47\text{dmpen})(\text{CH}_3\text{CN})]^+$ emitters). This behaviour, similar to that previously reported for $[\text{Re}(\text{CO})_3(\text{N}\text{O}\text{N})(\text{pyridine})]^+$ or $[\text{Re}(\text{CO})_3(\text{N}\text{O}\text{N})(\text{isonitrile})]^+$ complexes,^{41,42} can be explained assuming more or less pronounced mixing of the excited ${}^3\text{LC}$ (localized within NON ligands) and ${}^3\text{MLCT}$ states. The more energetic is the emission the smaller is the energy gap between the excited ${}^3\text{LC}$ and ${}^3\text{MLCT}$ states that leads to stronger mixing between them. Changing NON ligands one can tune the energy gap ΔE_{33} between the states involved in the electronic interaction because energies of the excited ${}^3\text{LC}$ and ${}^1\text{MLCT}/{}^3\text{MLCT}$ states depend on the ligand nature in different way. The introduction of the methyl substituent into 1,10-phenanthroline kernel shifts energies of the excited ${}^3\text{LC}$ and ${}^3\text{MLCT}$ states in the opposite directions (down and up, respectively) what results in the lowering of ΔE_{33} values. On the other hand, the presence of the phenyl groups attached to 1,10-phenanthroline kernel results in the parallel lowering of the excited ${}^3\text{LC}$ and ${}^3\text{MLCT}$ states energies. This effect is somewhat larger for ${}^3\text{LC}$, turning the photophysical properties of $[\text{Re}(\text{CO})_3(\text{dpphen})(\text{CH}_3\text{CN})]^+$ chelate distinctly different from that characteristic for $[\text{Re}(\text{CO})_3(\text{phen})(\text{CH}_3\text{CN})]^+$. These effects are considerably more important for the cationic $[\text{Re}(\text{CO})_3(\text{N}\text{O}\text{N})(\text{CH}_3\text{CN})]^+$ complexes what is reasonable taking into account the axial ligand induced the hypsochromic shift in their emission energies. Energies of the emissive ${}^3\text{MLCT}$ states E_{MLCT} are distinctly higher as compared with ${}^3\text{MLCT}$ states of $[\text{Re}(\text{CO})_3(\text{N}\text{O}\text{N})\text{Cl}]$.

The ligand induced changes in the spectroscopic and photophysical properties of the investigated chelates are also clearly seen in values of the emission quantum yields ϕ_{em} and the lifetimes of emission decays τ_{em} . Whereas the neutral $[\text{Re}(\text{CO})_3(\text{N}\text{O}\text{N})\text{Cl}]$ complexes are weakly emissive, their cationic $[\text{Re}(\text{CO})_3(\text{N}\text{O}\text{N})(\text{CH}_3\text{CN})]^+$ analogues belong to extremely efficient organometallic emitters. Similarly, very different values of the emission lifetime τ_{em} have been found for the investigated complexes (*cf.* Fig. 4). Due to the observed mono-exponential character of the ${}^3\text{MLCT}$ emission decays the

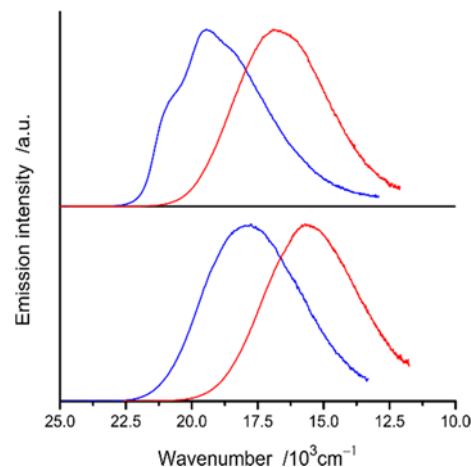


Fig. 3 Emission spectra of the neutral $[\text{Re}(\text{CO})_3(\text{N}\text{O}\text{N})\text{Cl}]$ (red lines) and cationic $[\text{Re}(\text{CO})_3(\text{N}\text{O}\text{N})(\text{CH}_3\text{CN})]^+$ (blue lines) complexes. Data for $\text{N}\text{O}\text{N} = 47\text{dmpen}$ (bottom) and dtbbpy (top).

radiative k_r and non-radiative k_{nr} rate constant values are directly related to the ${}^3\text{MLCT}$ emission quantum yields and lifetimes

$$k_r = \phi_{\text{em}} / \tau_{\text{em}} \quad (1a)$$

$$k_{\text{nr}} = (1 - \phi_{\text{em}}) / \tau_{\text{em}} \quad (1b)$$

and the resulting electronic transition dipole moments M_{em} values are given by⁴⁴

$$k_r = \frac{64\pi^4}{3h} (n\nu_{\text{em}}^{\text{max}})^3 |M_{\text{em}}|^2 \quad (2)$$

Deactivation of the excited ${}^3\text{MLCT}$ states of $[\text{Re}(\text{CO})_3(\text{N}\text{O}\text{N})(\text{CH}_3\text{CN})]^+$ is much slower as compared to their ${}^3\text{MLCT}$ counterparts. To some extent, it can be explained by the energy gap law, but the more detailed inspection of the values of radiative k_r and non-radiative k_{nr} rate constants leads to

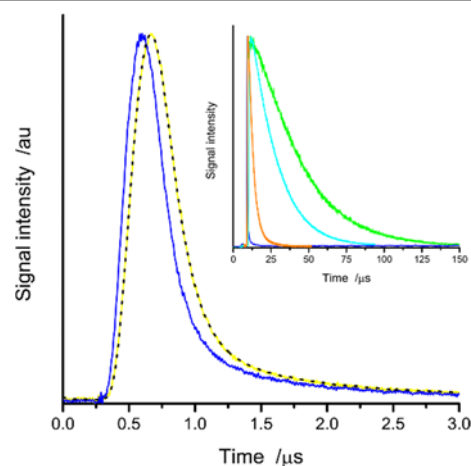


Fig. 4 Emission decay recorded for the neutral $[\text{Re}(\text{CO})_3(29\text{dmpen})\text{Cl}]$ chelate (yellow line) with the excitation pulse profile (blue line) and the fitted decay curve (dashed black line). Insert presents the long-lived emissions of the cationic $[\text{Re}(\text{CO})_3(\text{phen})(\text{CH}_3\text{CN})]^+$ (orange line), $[\text{Re}(\text{CO})_3(\text{tmphen})(\text{CH}_3\text{CN})]^+$ (blue line), and $[\text{Re}(\text{CO})_3(56\text{dmpen})(\text{CH}_3\text{CN})]^+$ (green line) complexes.

Table 2 Summary of the quantities describing $^3\text{MLCT} \rightarrow \text{S}_0$ emission from the excited $^3\text{MLCT} \rightarrow \text{S}_0$ states. The values of the outer λ_0 and inner λ_1 reorganization energies, the vibrational quanta $h\nu_1$, the Huang-Rhys factor S , the free energy gap E_{MLCT} as obtained from analysis of the MLCT emission band profiles, energy gap values between the NNN ligand centred ^3LC and $^3\text{MLCT}$ states ΔE_{33} , effective values of electronic coupling elements describing interactions between the excited $^3\text{MLCT}$ and ground S_0 states, experimental and computed k_{nr} values.

Complex type	Ligand NNN	λ_0 / eV	λ_1 / eV	$h\nu_1$ / eV	S	E_{MLCT} / eV	ΔE_{33} / eV	$V_{\text{eff}} / 10^{-3}$ eV	$k_{\text{nr}} / \text{s}^{-1}$	
									computed	experimental
[Re(CO)₃(NNN)(CH₃CN)]⁺										
	dpphen	0.26	0.27	0.16	1.69	2.57	0.02	11.1	3.0×10^4	3.5×10^4
	bpy	0.37	0.28	0.18	1.56	2.67	0.21	32.0	3.3×10^6	1.5×10^6
	dbbpy	0.36	0.29	0.18	1.61	2.72	0.11	34.4	2.7×10^6	1.1×10^6
	phen	0.38	0.23	0.19	1.21	2.70	0.05	22.3	3.9×10^5	2.0×10^5
	29dmphen	0.27	0.32	0.17	1.88	2.72	0.03	17.8	2.5×10^5	5.1×10^5
	56dmphen	0.18	0.32	0.17	1.88	2.62	-0.02	6.2	2.5×10^4	1.4×10^4
	47dmphen	0.13	0.34	0.17	2.00	2.69	-0.02	7.9	1.7×10^4	7.6×10^4
	tmphen	0.13	0.35	0.17	2.06	2.70	-0.01	7.1	1.7×10^4	4.9×10^4
[Re(CO)₃(NNN)Cl]										
	dpphen	0.45	0.22	0.18	1.22	2.41	0.18	22.0	1.1×10^6	3.0×10^6
	bpy	0.45	0.21	0.18	1.17	2.45	0.43	24.7	6.0×10^7	2.1×10^7
	dbbpy	0.49	0.24	0.18	1.33	2.51	0.32	28.5	2.2×10^7	1.1×10^7
	phen	0.53	0.20	0.18	1.11	2.53	0.22	26.6	6.2×10^6	6.5×10^6
	29dmphen	0.52	0.22	0.18	1.22	2.56	0.19	31.0	1.1×10^7	1.4×10^7
	56dmphen	0.46	0.20	0.18	1.11	2.48	0.12	22.8	2.8×10^6	4.2×10^6
	47dmphen	0.45	0.26	0.18	1.44	2.58	0.09	20.3	5.8×10^6	1.5×10^6
	tmphen	0.47	0.22	0.18	1.22	2.63	0.06	17.5	7.1×10^5	4.7×10^5

conclusion that the energy of the given emitter E_{MLCT} is not a single factor controlling its radiative and non-radiative deactivation. Comparing $[\text{Re}(\text{CO})_3(\text{dpphen})(\text{CH}_3\text{CN})]^+$ with $[\text{Re}(\text{CO})_3(\text{bpy})(\text{CH}_3\text{CN})]^+$ as well as $[\text{Re}(\text{CO})_3(\text{dpphen})\text{Cl}]$ with $[\text{Re}(\text{CO})_3(\text{bpy})\text{Cl}]$ one can clearly see the essential difference between the complexes with dpphen and bpy ligands despite that their emission maxima $\tilde{\nu}_{\text{em}}^{\text{max}}$ are located at nearly the same wavenumbers.

Emission band shape analysis

An additional information on the properties of the excited $^1\text{MLCT}$ and $^3\text{MLCT}$ states can be obtained from the band shape analysis of the charge transfer absorption $^1\text{MLCT} \leftarrow \text{S}_0$ and/or emission $^3\text{MLCT} \rightarrow \text{S}_0$. The absorption band profile, *i.e.*, the relationship between the molar absorption coefficient $\varepsilon_{\text{M}}(\tilde{\nu}_{\text{abs}})$ and the absorbed photon energy $hc\tilde{\nu}_{\text{abs}}$ can be expressed as follows⁴⁶⁻⁴⁹

$$\frac{\varepsilon_{\text{M}}(\tilde{\nu}_{\text{abs}})}{n\tilde{\nu}_{\text{abs}}} = \frac{8\pi^3}{3\ln 10} \frac{M_{\text{abs}}^2}{c} \sum_{j=0}^{\infty} \frac{e^{-S} S^j}{j!} \times \exp\left[-\frac{(E_{\text{MLCT}} + \lambda_0 + jh\nu_1 - hc\tilde{\nu}_{\text{abs}})^2}{4\lambda_0 k_{\text{B}} T}\right] \quad (3)$$

where n , c , k_{B} , and T are the solvent refraction index, light velocity, the Boltzmann constant, and absolute temperature, respectively. In a similar way, the MLCT emission profile, *i.e.*, the relationship between the emission intensity $I(\tilde{\nu}_{\text{em}})$ (in photons per second per unit of spectral energy) and the emitted photon energy $hc\tilde{\nu}_{\text{em}}$ is given by⁵⁰⁻⁵²

$$\frac{I(\tilde{\nu}_{\text{em}})}{(n\tilde{\nu}_{\text{em}})^3} = \frac{64\pi^4}{3h} M_{\text{em}}^2 \sum_{j=0}^{\infty} \frac{e^{-S} S^j}{j!} \times \exp\left[-\frac{(E_{\text{MLCT}} - \lambda_0 - jh\nu_1 - hc\tilde{\nu}_{\text{em}})^2}{4\lambda_0 k_{\text{B}} T}\right] \quad (4)$$

where h denotes the Planck constant. In both of the above relationships the electron-vibration coupling constant, the Huang-Rhys factor S , is equal to the inner reorganization energy λ_1 expressed in units of vibrational quanta $h\nu_1$ ($S = \lambda_1 / h\nu_1$). The inner reorganization energy λ_1 corresponds to the high-frequency motions (represented by a single "averaged" mode characterized by $h\nu_1$) associated with the intra-ligand changes in the bond lengths and angles. The outer reorganization energy λ_0 is related to the low- and medium-frequency motions (reorientation of the solvent shell, changes in the metal-ligands bond lengths, *etc.*) accompanying the electron transfer. According to the above two equations the Franck-Condon factor for the MLCT absorption processes differs from that for the MLCT emission process only in the sign of the $\lambda_0 + jh\nu_1$ term. Thus one can expect a mirror image between the normalized, so called reduced $\varepsilon(\tilde{\nu}_{\text{abs}})/\tilde{\nu}_{\text{abs}}$ and $I(\tilde{\nu}_{\text{em}})/\tilde{\nu}_{\text{em}}^3$ spectra. Of course, strictly mirror image behaviour could be only observed if all intrinsic, E_{MLCT} , λ_0 , λ_1 , and $h\nu_1$ quantities are exactly the same for both $^1\text{MLCT} \leftarrow \text{S}_0$ and $^3\text{MLCT} \rightarrow \text{S}_0$ processes (the case of nearly degenerated $^1\text{MLCT}$ and $^3\text{MLCT}$, both with 100% MLCT character). Usually, it is not a case due to the differences in the electronic interactions between the excited $^1\text{MLCT}$ and ^1LC or $^3\text{MLCT}$ and ^3LC states.

The results from the performed band shape analyses are collected in Table 2. Representative examples of the numerical

fits (presented in Fig. 5) show that the experimental MLCT emission profiles of all the *fac*-Re(CO)₃⁺ chelates studied could be adequately reproduced within a single high-frequency mode approximation. It should be noted, however, that E_{MLCT} and λ_0 as well as λ_1 and $h\nu_1$ quantities turn out to be somewhat correlated, leading to a numerical uncertainty (± 0.02 eV) of their fitted values. Due to the applied model approximations, however, the real uncertainty can be still larger, for example as a consequence of assumption that the M_{em} value is independent of the emitted photon energy. Moreover neglecting of a medium-frequency mode contributions leads to the small overestimation of the fitted E_{MLCT} and λ_0 quantities. Despite of all simplifications in the formalism used to fit the band profiles of the experimentally observed $^3\text{MLCT} \rightarrow \text{S}_0$ emission spectra some conclusions, however, can be drawn based on the data from the performed band shape analyses. First of all, the same set of E_{MLCT} , λ_0 , λ_1 , and $h\nu_1$ parameters can be further used in discussion of the non-radiative $^3\text{MLCT} \rightarrow \text{S}_0$ transition.

Due to the analogy between the CT optical spectroscopy and the thermal electron transfer processes, values of non-radiative k_{nr} rate constants can be predicted (within the framework of semi-classical approach) from the following expression⁵³⁻⁵⁶

$$k_{\text{nr}} = \frac{4\pi^2}{h} \frac{V_{\text{eff}}^2}{\sqrt{4\pi\lambda_0 k_{\text{B}}T}} \sum_{j=0}^{\infty} \frac{e^{-S} S^j}{j!} \times \exp\left[-\frac{(E_{\text{MLCT}} - \lambda_0 - jh\nu_1)^2}{4\lambda_0 k_{\text{B}}T}\right] \quad (5)$$

Thus the data derived from the band-shape analysis of the MLCT emission spectra can be used to reproduce the experimentally found k_{nr} rate constants when the “effective” values of electronic coupling element V_{eff} describing the electronic interaction between the excited $^3\text{MLCT}$ and ground S_0 states become available from any other experimental data. In the case of radiative CT processes the electronic coupling elements V can be obtained from the experimental values of the electronic transition dipole moments M_{abs} and M_{em} in terms of the Mulliken model originally developed for the CT complexes.^{57,58} Within this models M_{abs} and M_{em} are related to the electronic coupling matrix element for the thermal electron transfer, V_{CT} , via the change in dipole moment $\Delta\mu$ associated with the electron transfer and the energy gap ΔE between the states involved in these processes. Thus in the case of MLCT systems the observed M_{abs} value characterizing the spin-allowed radiative $^1\text{MLCT} \leftarrow \text{S}_0$ transition can be expressed as follows

$$M_{\text{abs}} = \frac{V_{\text{CT}}}{hc\nu_{\text{abs}}} \Delta\mu \quad (6)$$

whereas in the case of the spin-forbidden radiative $^3\text{MLCT} \rightarrow \text{S}_0$ transition the mixing between the excited $^1\text{MLCT}$ and $^3\text{MLCT}$ states, proportional to the spin-orbit coupling V_{SOC} and inversely proportional to the energy gap ΔE_{ST} between them, is additionally taken into account^{59,60}

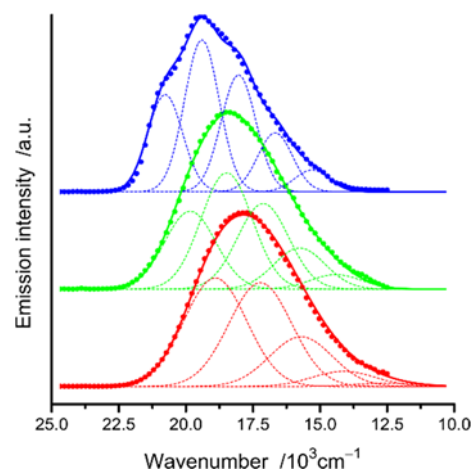


Fig. 5 $^3\text{MLCT} \rightarrow \text{S}_0$ luminescence spectra of $[\text{Re}(\text{CO})_3(\text{tmphen})(\text{CH}_3\text{CN})]^+$ (blue circles), $[\text{Re}(\text{CO})_3(29\text{dmphen})(\text{CH}_3\text{CN})]^+$ (green circles), and $[\text{Re}(\text{CO})_3(\text{dtbbpy})(\text{CH}_3\text{CN})]^+$ (red circles) complexes and the corresponding numerical fits (solid lines) according to eq. 4. Dashed lines show contributions from the individual vibronic transitions. Six vibronic transitions ($0 \rightarrow 0$, $0 \rightarrow 1$, $0 \rightarrow 2$, etc.) have been taken into account. Only five of them can be seen in the presented figures because very low, marginal contribution from the vibronic transitions with $j \geq 5$.

$$M_{\text{em}} = \frac{V_{\text{SOC}}}{\Delta E_{\text{ST}}} \frac{V_{\text{CT}}}{hc\nu_{\text{em}}} \Delta\mu = \frac{V_{\text{eff}}}{hc\nu_{\text{em}}} \Delta\mu \quad (7)$$

Both equations are only valid if contribution from the locally excited ^1LC configurations can be neglected.⁶¹⁻⁶³ However, due to relatively large energy gap between the excited ^1LC and $^3\text{MLCT}$ states, one can use equation 7 (at least in the first-order approximation) in estimation of V_{eff} terms from the experimentally available M_{em} values. The experimentally found M_{em} values (data in Table 1) together with the assumed $\Delta\mu = 15$ D lead to V_{eff} values (data in Table 2) further used to compute k_{nr} rate constants according to equation 5. The results of the performed calculations are summarized in Table 2 and illustrated in Fig. 6. The discrepancies between the experimentally found and computed rate constants k_{nr} are not

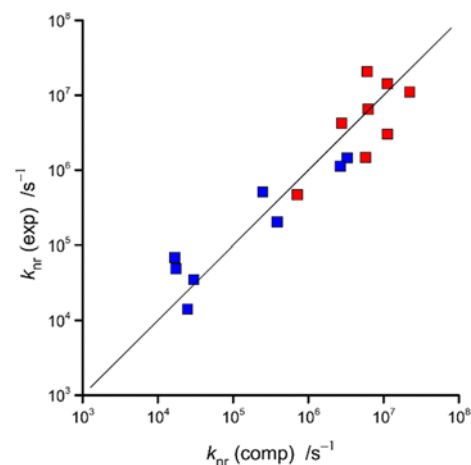


Fig. 6 Relation between the computed and experimental values of non-radiative k_{nr} rate constants of $^3\text{MLCT} \rightarrow \text{S}_0$ transitions for the investigated $[\text{Re}(\text{CO})_3(\text{NON})\text{Cl}]$ (red symbols) and $[\text{Re}(\text{CO})_3(\text{NON})(\text{CH}_3\text{CN})]^+$ (blue symbols) complexes.

exceeding a factor 3-4 that may be regarded as more than satisfactory. The obtained agreement allow us also to assume that the fitted E_{MLCT} , λ_0 , λ_1 , and $h\nu_i$ quantities have been properly estimated and their values can be used for further discussion.

An additional possibility to test self-consistency of the fitted E_{MLCT} , λ_0 , λ_1 , and $h\nu_i$ parameters arises from the expected mirror image between the MLCT absorption and emission spectra. Comparing the experimentally found values of the transition dipole moments M_{abs} and M_{em} (data in Table 1) describing both types of the investigated transitions one can expect that the f values (and ϵ_{M} correspondingly) for the spin-allowed $^1\text{MLCT} \leftarrow \text{S}_0$ *ca.* are two orders of magnitude larger than characterizing the spin-forbidden $^3\text{MLCT} \leftarrow \text{S}_0$ transition. This makes direct observation of the $^3\text{MLCT} \leftarrow \text{S}_0$ absorption band in the ordinary UV-vis spectra hardly possible. However, using the fitted E_{MLCT} , λ_0 , λ_1 , and $h\nu_i$ quantities, one can predict shape and position of the $^3\text{MLCT} \leftarrow \text{S}_0$ bands, not observed experimentally due to small values of the oscillator strength f characterizing these transitions. Examples of the “hypothetical” $^3\text{MLCT} \leftarrow \text{S}_0$ bands are depicted in Fig. 7 together with the experimentally found $^1\text{MLCT} \leftarrow \text{S}_0$ spectra. As expected, both bands are localized in the nearly same spectral region making a separation of $^3\text{MLCT} \leftarrow \text{S}_0$ transitions from *ca.* hundred times more intense $^1\text{MLCT} \leftarrow \text{S}_0$ band really impossible. As expected (*cf.* the right chart in Figure 8), small bathochromic shift between $^1\text{MLCT} \leftarrow \text{S}_0$ and $^3\text{MLCT} \leftarrow \text{S}_0$ transition can be clearly seen. The observed shift 1700-2300 cm^{-1} (*ca.* 0.2-0.3 eV) can be very roughly attributed to the energy splitting ΔE_{ST} between the excited $^1\text{MLCT}$ and $^3\text{MLCT}$ states. It should be noted, however, that, due to systematic errors, especially in the estimation of E_{MLCT} and λ_0 values (*vide infra*) the resulting ΔE_{ST} values are extremely imprecise.

Inner and outer reorganization energies

As mentioned above, neglecting of a medium-frequency mode contribution may lead to the parallel over-estimation of E_{MLCT} and λ_0 values when the simplified one high-frequency mode approximation is used in the procedures applied to fit emission spectra. However, this can be to some extent overcome as it has been proposed by Cortes, Heitele, and Jortner.⁶⁴ Their approach, based on the semi-classical treatment of the medium-frequency modes together with the classical and quantum treatment of the low-frequency and high-frequency modes, respectively, leads to reformulation of equations 3, 4 and 5 through simple modification of the denominator in the exponential parts of these equations. Due to contribution of the medium-frequency modes $h\nu_{\text{M}}$ (associated with the reorganization energy λ_{M}) the original $4\lambda_0 k_{\text{B}}T$ denominator should be replaced by $4k_{\text{B}}T\lambda_1 + 2h\nu_{\text{M}}\lambda_{\text{M}}\coth[h\nu_{\text{M}}/2k_{\text{B}}T]$ term. The proposed modification arises from dividing of the outer reorganization energy λ_0 into contribution of the low-frequency (mainly solvent) and the medium-frequency modes (mainly solute) associated with the reorganization energies λ_{M} and λ_1 respectively. In view of the introduced modification of the denominator one can correct the fitted E_{MLCT} and λ_0 values

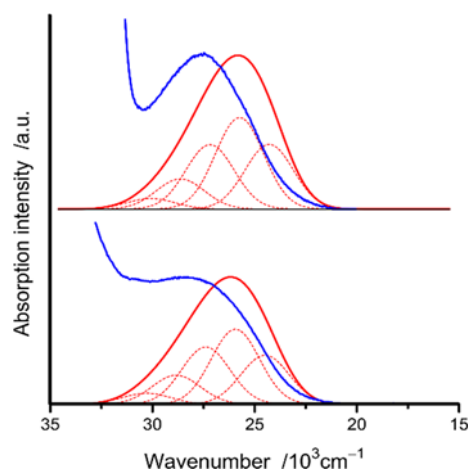


Fig. 7 Profiles of the experimentally observed $^1\text{MLCT} \leftarrow \text{S}_0$ (blue lines) and “hypothetical” $^3\text{MLCT} \leftarrow \text{S}_0$ (red lines) absorption bands for $[\text{Re}(\text{CO})_3(\text{dtbbpy})\text{Cl}]$ (top) and $[\text{Re}(\text{CO})_3(47\text{dmphen})\text{Cl}]$ (bottom) complexes. Dashed lines show contributions from the individual vibronic transitions. Six vibronic transitions ($0 \rightarrow 0$, $0 \rightarrow 1$, $0 \rightarrow 2$, etc.) have been taken into account. Only five of them can be seen in the presented figures because very low, marginal contribution from the vibronic transitions with $j \geq 5$.

(without performing any additional fits) according to the following relations⁶⁴

$$\lambda_0(\text{fit}) - \lambda_0(\text{true}) = \lambda_{\text{M}} \left[1 - \frac{2k_{\text{B}}T}{h\nu_{\text{M}}} \tanh \left[\frac{h\nu_{\text{M}}}{2k_{\text{B}}T} \right] \right] \quad (8a)$$

and

$$E_{\text{MLCT}}(\text{fit}) - E_{\text{MLCT}}(\text{true}) = \lambda_{\text{M}} \left[1 - \frac{2k_{\text{B}}T}{h\nu_{\text{M}}} \tanh \left[\frac{h\nu_{\text{M}}}{2k_{\text{B}}T} \right] \right] \quad (8b)$$

The corresponding corrections depend on λ_{M} and $h\nu_{\text{M}}$ values. For typical value of the medium-frequency mode $h\nu_{\text{M}} = 0.050$ eV (400 cm^{-1}) the right side term in equations 8a and 8b is equal to *ca.* 20% of λ_{M} . For a more detailed analysis, an additional information about relative contributions of λ_1 and λ_{M} are necessary for estimation of the appropriate corrections. This information could be available from any more advanced (*e.g.*, temperature effect on emission spectra^{64,65}), studies. The already available data allow only estimation of the upper limit of these corrections. Taking into account the fitted λ_0 values one can conclude that the correction are relatively small, ranging from *ca.* 0.02-0.03 eV for the cationic $[\text{Re}(\text{CO})_3(\text{tmphen})(\text{CH}_3\text{CN})]^+$ or $[\text{Re}(\text{CO})_3(47\text{dmphen})(\text{CH}_3\text{CN})]^+$ chelates up to maximally *ca.* 0.1 eV for the neutral $[\text{Re}(\text{CO})_3(\text{N}\cap\text{N})\text{Cl}]$ species. It means that the “true” values of the energy gaps ΔE_{33} between the excited ^3LC and $^3\text{MLCT}$ states within the investigated *fac*- $\text{Re}(\text{CO})_3^+$ chelates are somewhat more positive than presented in Table 2. In a similar way the “true” λ_0 values are somewhat smaller than the fitted ones. However, because the corrections are small, all the observed trends (*e.g.*, monotonic relationship between ΔE_{33} and λ_0 values) remain essentially unaffected.

For all the complexes under study the average quantum spacing, $h\nu_i$ is in the range of 0.16-0.19 eV (1300 - 1550 cm^{-1}). Nearly constant $h\nu_i$ value (contributions from the vibrational

modes of $\text{N}\equiv\text{C}$, $\text{N}=\text{C}$, and $\text{C}=\text{C}$ bond stretching) reflects a similar ligands environment around the central $\text{fac-Re}(\text{CO})_3^+$ core. Values of the inner reorganization energies, λ_i (and the Huang-Rhys factors S) depend to some extent on the nature of the given emitter. Interestingly, in the case of neutral $[\text{Re}(\text{CO})_3(\text{N}\text{ON})\text{Cl}]$ chelates the found λ_i values (0.20–0.26 eV) are markedly smaller than those characteristic for their ionic $[\text{Re}(\text{CO})_3(\text{N}\text{ON})(\text{CH}_3\text{CN})]^+$ analogues (up to 0.35 eV). Most probably the effect is connected with different nature of the neutral $\text{Re}(\text{CO})_3\text{Cl}$ and ionic $\text{Re}(\text{CO})_3(\text{CH}_3\text{CN})^+$ fragments participating in the electron transfer process associated with the MLCT excitation. In the case of studied complexes an electron is transferred from $\text{Re}(\text{I})$ ion to NON ligand. Thus the MLCT excitation process corresponds to the intramolecular oxidation of $\text{Re}(\text{I})$ to $\text{Re}(\text{II})$ that forces changes in the $\text{Re}-\text{C}$ and $\text{C}\equiv\text{N}$ bonds. Such changes should be more pronounced in the case of ionic $[\text{Re}(\text{CO})_3(\text{N}\text{ON})(\text{CH}_3\text{CN})]^+$ complexes where the charge on the central rhenium atom changes actually from +1 to +2. In the case of neutral $[\text{Re}(\text{CO})_3(\text{N}\text{ON})\text{Cl}]$ complexes, due to the covalent character of $\text{Re}-\text{Cl}$ bond, the central ion charge changes apparently from 0 to +1. The above considerations about changes of charge on $\text{Re}(\text{CO})_3\text{Cl}$ or $\text{Re}(\text{CO})_3(\text{CH}_3\text{CN})^+$ kernels remain also valid when strong electronic interactions between the excited $^3\text{MLCT}$ and ^3LC states take place. In such the case the effective charge changes from 0 to +0.5–1 or +1 to +1.5–2 are expected still to diversify the investigated $[\text{Re}(\text{CO})_3(\text{N}\text{ON})\text{Cl}]$ and $[\text{Re}(\text{CO})_3(\text{N}\text{ON})(\text{CH}_3\text{CN})]^+$ complexes. Thus the observed differences in the fitted λ_i values can be rationalized with regards to different ability of CO ligand to coordinate the low and high valence metal ions. Similar effects should be observed in any electron transfer processes involving $\text{fac-Re}(\text{CO})_3^+$ complexes. Their rates should be smaller in the case of $\text{Re}(\text{CO})_3(\text{CH}_3\text{CN})^+$ derivatives due to larger (as compared to these containing $\text{Re}(\text{CO})_3\text{Cl}$ kernel) values of λ_i energies. In fact, it has been observed in the electrochemical studies^{66–69} of $[\text{Re}(\text{CO})_3(\text{N}\text{ON})(\text{CH}_3\text{CN})]^+$ and $[\text{Re}(\text{CO})_3(\text{N}\text{ON})\text{Cl}]$ complexes. Whereas the electrochemical oxidation of

$[\text{Re}(\text{CO})_3(\text{N}\text{ON})(\text{CH}_3\text{CN})]^+$ species is usually slow and electrochemically quasi-reversible, the analogous processes involving $[\text{Re}(\text{CO})_3(\text{N}\text{ON})\text{Cl}]$ chelates are much faster exhibiting the electrochemical reversibility as it can be deduced from the observed difference in the anodic and cathodic peaks potentials on the recorded cyclic voltammetry curves.

Another, well pronounced trend can be seen in the relation between the fitted λ_0 and ΔE_{33} values. The observed behaviour can be rationalized in terms of the excited ^3LC and $^3\text{MLCT}$ states mixing governed by the energy gap between them. This can be roughly estimated taking into account the energies of the 0–0 transition in the phosphorescence spectra of free NON ligands^{70,71} and the E_{MLCT} energies available from the performed fitting of the $^3\text{MLCT} \rightarrow \text{S}_0$ emission band profiles. The larger the energy gap between the excited $^3\text{MLCT}$ and ^3LC states, ΔE_{33} , the larger the observed λ_0 value. It arises from different contribution of the excited ^3LC state to the wavefunction characterizing the given $^3[\text{Re}(\text{CO})_3(\text{N}\text{ON})(\text{CH}_3\text{CN})]^+$ or $^3[\text{Re}(\text{CO})_3(\text{N}\text{ON})\text{Cl}]$ emitter. When the excited $^3\text{MLCT}$ and ^3LC states are close in energy, the resulting emitter is characterized by an equivalent contribution of them. It results in lowering of the outer reorganization energy λ_0 to *ca.* $\frac{1}{4}$ of that characterizing “100% pure” MLCT state. It is indeed observed in the case of studied $\text{fac-Re}(\text{CO})_3^+$ chelates with λ_0 ranging from 0.13 to 0.53 eV for the smallest and largest ΔE_{33} values, respectively. Whereas λ_0 depends monotonically on ΔE_{33} , changes in λ_i do not follow the same trend. It arises from similar λ_i values for both of the mixing ^3LC and $^3\text{MLCT}$ configuration and distinctly different λ_0 values characterizing “pure” $^3\text{LC} \rightarrow \text{S}_0$ and $^3\text{MLCT} \rightarrow \text{S}_0$ transitions.

Electronic and spin-orbit coupling elements

Data available from the performed band shape analyses allow also for more or less accurate discussion of the potential energy curves describing adiabatic/non-adiabatic transitions between the excited ^3LC and $^3\text{MLCT}$ or ^1LC and $^1\text{MLCT}$ states. Less accurate when necessary values of the electronic coupling

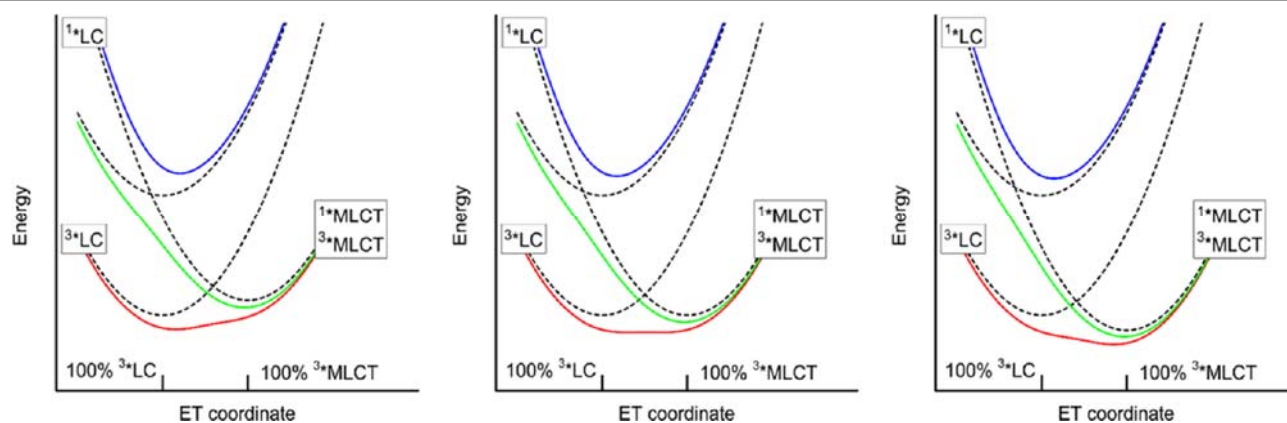


Fig. 8 Potential energy curves of the ligand centred ^1LC , ^3LC , and $^1,^3\text{MLCT}$ excited states. Dashed lines represent the initial states whereas solid lines correspond to the resulting states due to electronic interaction between them. Green and blue solid lines are related to the resulting diabatic $^1\text{MLCT}$ state and the lowest ^1LC state, whereas the red solid line shows the adiabatic transition from the lowest excited ^3LC state to $^3\text{MLCT}$ state, respectively. Pictures correspond to different energy gaps between the initial ^3LC and MLCT states, -0.1 eV (left), 0 eV (middle), and $+0.1$ eV (right), respectively (negative and positive signs of the energy gap denote localization of the $^3\text{MLCT}$ state above ^3LC state). Potential energy curves were simulated with $\lambda_0 = 0.55$ eV (assumed for 100% “pure” MLCT configuration) and $V_{33} = V_{11} = 0.25$ eV. Value of 0.8 eV was taken as energy gap between the excited ^1LC and ^3LC states.

elements V are arbitrary chosen, and more accurate (as it is presented in Fig. 8) when their values are experimentally accessed. Fortunately, in the case of complexes under investigations the already available photophysical data allow quite precise estimation of the necessary quantities: the V_{CT} values describing the spin-allowed interactions between the excited $^1\text{MLCT}$ and the ground states S_0 as well as the V_{33} values responsible for the electronic interactions between the excited $^3\text{MLCT}$ and ^3LC states.

To evaluate V_{CT} value one can consider the estimated values of the transition dipole moments M_{abs} describing the $^1\text{MLCT} \leftarrow S_0$ transitions. According to Eq. 6 one can obtain V_{CT} values from the experimental M_{abs} and $hc\tilde{\nu}_{abs}^{\sim\max}$ data collected in Table 1. The resulting $V_{CT} = 0.3\text{--}0.6$ eV must be, however, treated as the upper limit estimates because the applied procedure neglects plausible contribution of the intensity borrowing from the $^1\text{LC} \leftarrow S_0$ transitions and possible overestimations of the M_{abs} caused by partial overlapping of $^1\text{MLCT} \leftarrow S_0$ and $^1\text{LC} \leftarrow S_0$ absorption bands.

The V_{33} values can be accessed taking into account the position of the 0–0 transition in the structured emission spectra of $fac\text{-Re}(\text{CO})_3^+$ complexes exhibiting $^3\text{LC} \rightarrow S_0$ transitions. Position of the 0–0 transitions in the $^3\text{LC} \rightarrow S_0$ emission in these complexes is, as compared to the isolated $\text{N}\wedge\text{N}$ ligands, bathochromically shifted due to the electronic interactions between the excited ^3LC and, higher energetically located, $^3\text{MLCT}$ state. The observed shift $hc\Delta\tilde{\nu}_{0-0}$ can be related to the energy gap between the excited $^3\text{MLCT}$ and ^3LC states, approximated by the difference in the $^3\text{LC} \rightarrow S_0$ emission and $^3\text{MLCT} \leftarrow S_0$ (or nearly iso-energetic $^1\text{MLCT} \leftarrow S_0$) absorption maxima as follow

$$hc\Delta\tilde{\nu}_{0-0} = \frac{V_{33}^2}{hc\tilde{\nu}_{abs}^{\sim\max} - hc\tilde{\nu}_{em}^{\sim\max}} \quad (9)$$

In estimation of the V_{33} values one can use results from the measurements performed at 77 K if the medium rigidity effect are large enough to change the energetic sequence of the excited $^3\text{MLCT}$ and ^3LC states and the character of the observed emission. Alternatively, and still better, one can use photophysical data for some similar $fac\text{-Re}(\text{CO})_3^+$ complexes exhibiting the $^3\text{LC} \rightarrow S_0$ type emission in the fluid media at room temperature. Although this is not a case for the studied complexes, some of their analogues, namely $[\text{Re}(\text{CO})(\text{N}\wedge\text{N})(\text{RNC})]^+$ chelates in which the axial CH_3CN ligand is replaced by an aliphatic isonitrile, exhibit the $^3\text{LC} \rightarrow S_0$ type emission at such conditions.⁴² With the observed $hc\Delta\tilde{\nu}_{0-0}$ values (being equal to *ca.* 0.08–0.09 eV for $[\text{Re}(\text{CO})_3(47\text{dmphen})(t\text{-BuNC})]^+$ or $[\text{Re}(\text{CO})_3(\text{tmphen})(t\text{-BuNC})]^+$ species), and the estimated $hc\tilde{\nu}_{abs}^{\sim\max} - hc\tilde{\nu}_{em}^{\sim\max}$ terms (in the range of *ca.* 0.8–1.0 eV) the resulting $V_{33} \approx 0.2\text{--}0.3$ eV are close to the lower limit of the previously discussed V_{CT} quantities.

The remaining V_{11} values, describing the spin-allowed interactions between the excited $^1\text{MLCT}$ and ^1LC states, is not directly accessible but, at least in the first order approximation, one can assume $V_{11} \approx V_{33}$. Assumption about comparable values of these electronic coupling terms is based on the Dogonadze

concept⁷² relating the electronic coupling between the central metal ion and the attached ligand(s) to the nature of the frontier orbitals involved in these interactions. Due to the similar values of the LCAO coefficients describing the frontier orbital of α -diimine ligand, either for the isolated $\text{N}\wedge\text{N}$ molecules (*e.g.*, from semi-empirical calculations) as well as for the attached to $fac\text{-Re}(\text{CO})_3^+$ core (*e.g.*, from DFT calculations⁷³), one can anticipate $V_{11} \approx V_{33}$ and $V_{11} \approx V_{CT}$. It should be also emphasized that precise knowledge of V_{11} values is much less essential for the discussed issue because the electronic interactions between the excited ^1LC and $^1\text{MLCT}$ state are only weakly affecting the $^3\text{MLCT}/^3\text{LC}$ or $^3\text{MLCT}/S_0$ relations.

As mentioned above, the estimated values of the electronic coupling elements together with the energetic ΔE_{33} and λ_0 parameters available from the performed emission band shape analyses allow us a more quantitative discussion of the potential energy curves describing the investigated MLCT systems. Due to relatively large V_{33} values, larger than $\lambda_0/4$ terms, shape of the potential energy curve, resulting from the electronic interaction between the initial “pure” ^3LC and $^3\text{MLCT}$ states, strongly depends on the energy gap between them. Contrary to that, shapes of the potential energy curve of the initial “pure” $^1\text{MLCT}$ and ^1LC state remains much less affected, mostly due to larger energy gaps between the excited ^1LC and $^1\text{MLCT}$ or $^1\text{MLCT}$ and S_0 states, respectively. Moreover, the both types of the electronic interactions affecting energy of the excited $^1\text{MLCT}$ state are working in the opposite direction that to a large extent cancels their energetic contributions.

Electronic interactions between the excited $^3\text{MLCT}$ and ^3LC states are distinctly more pronounced than those characterizing the semi-detached $^1\text{MLCT}/^1\text{LC}/S_0$ systems. It leads to quite different shapes of the potential energy curves describing the singlet and triplet states possessing MLCT character and the energy gap ΔE_{ST} between them. The latter is particularly important because ΔE_{ST} affects strongly the mixing between the excited $^1\text{MLCT}$ and $^3\text{MLCT}$ states that results in appropriate changes of values of the transition dipole moment M_{em} values characterizing the $^3\text{MLCT} \rightarrow S_0$ emission (*cf.* equation 7). For the given MLCT emitter ΔE_{ST} can be related to the sum of ΔE_{33} and λ_0 terms that are directly available from the emission band shape analyses.

$$\Delta E_{ST} = \frac{V_{33}^2}{\Delta E_{33} + \lambda_0} \quad (10)$$

Although both ΔE_{33} and λ_0 values are somewhat overestimated, the estimation errors (the same for both quantities) cancel in the calculation of the vertical energy gaps $\Delta E_{33} + \lambda_0$ between the excited $^1\text{MLCT}$ and $^3\text{MLCT}$ states with the solvent/solute conformation characteristic for the equilibrated conformation of the emissive $^3\text{MLCT}$ species.

The energy splitting ΔE_{ST} between the excited $^3\text{MLCT}$ and $^1\text{MLCT}$ states depends inversely on the sum of two terms, the energy gap ΔE_{33} between the lowest excited ^3LC (within the α -diimine N ligand) and the outer reorganization energy λ_0 . The smaller the sum $\Delta E_{33} + \lambda_0$ the larger the ΔE_{ST} difference what

results in less pronounced mixing between the excited $^3\text{MLCT}$ and $^1\text{MLCT}$ states. Because λ_0 depends also on ΔE_{33} , one can observe (as it is presented in this work) quite huge changes in the observed values of k_r and k_{nr} rate constants despite that very similar NN ligands are present in the investigated $[\text{Re}(\text{CO})_3(\text{N}\text{N})\text{Cl}]$ or $[\text{Re}(\text{CO})_3(\text{N}\text{N})(\text{CH}_3\text{CN})]^+$ complexes. For the studied complexes one can estimate ΔE_{ST} values using the experimentally affordable parameters. With the electronic coupling value $V_{33} \approx 0.25\text{--}0.30$ eV and the sum $\Delta E_{33} + \lambda_0$ in the range of 0.11–0.88 eV (*cf.* data in Table 2) one can obtain ΔE_{ST} as small as 0.07–0.10 eV (*e.g.*, $[\text{Re}(\text{CO})_3(\text{bpy})\text{Cl}]$ chelate) or as large as 0.57–0.82 eV (*e.g.*, $[\text{Re}(\text{CO})_3(\text{tmphen})(\text{CH}_3\text{CN})]^+$ chelate). Nearly one order of magnitude large span of the estimated ΔE_{ST} values clarifies the observed differences in the emissive properties of the studied *fac*- $\text{Re}(\text{CO})_3^+$ complexes. The ΔE_{ST} values estimated for $[\text{Re}(\text{CO})_3(\text{dtbbpy})\text{Cl}]$ (0.08–0.11 eV) and $[\text{Re}(\text{CO})_3(47\text{dmphen})\text{Cl}]$ (0.12–0.17 eV) complexes are somewhat smaller than those anticipated (0.2–0.3 eV) from the differences between their absorption maxima of $^1\text{MLCT} \leftarrow \text{S}_0$ (experimental) and $^3\text{MLCT} \leftarrow \text{S}_0$ (simulated) transitions (*cf.* Figure 7). However, taking into account all possible errors and approximations made, the agreement can be regarded as satisfactory.

The ΔE_{ST} values characterizing the investigated *fac*- $\text{Re}(\text{CO})_3^+$ complexes can be used to discuss the experimental values of the transition dipole moment M_{em} of $^3\text{MLCT} \leftarrow \text{S}_0$ transitions. By combining equation (7) with equation (10) one can obtain

$$M_{\text{em}} = \frac{V_{\text{SOC}} V_{\text{CT}}}{V_{33}^2} \times \frac{\Delta E_{33} + \lambda_0}{h c \nu_{\text{em}}^{\text{max}}} \Delta \mu \quad (11)$$

According to the above equation the transition dipole moments M_{em} should increase with value of $\Delta E_{33} + \lambda_0$ term. It can be indeed seen comparing appropriate data in Tables 1 and 2. Optionally one can directly predict the M_{em} values when necessary parameter V_{SOC} is available, *e.g.*, from the quantum

mechanical calculation or any other photophysical data. According to results from the DFT calculation V_{SOC} values are equal 0.011 eV for one of the investigated neutral $[\text{Re}(\text{CO})_3(\text{bpy})\text{Cl}]$ complexes and the 0.0072 eV for the analogous cationic $[\text{Re}(\text{CO})_3(4\text{-ethylpyridine})]^+$ complex.⁷⁴ With the averaged $V_{\text{SOC}} = 0.0091$ eV one can obtain value of $V_{\text{SOC}} V_{\text{CT}} \Delta \mu / V_{33}^2$ term (0.683 D^{-1} with $\Delta \mu = 15$ D and $V_{\text{CT}} = V_{33} = 0.2$ eV or 0.455 D^{-1} when $V_{\text{CT}} = V_{33} = 0.3$ eV). With the intermediate $V_{\text{SOC}} V_{\text{CT}} \Delta \mu / V_{33}^2 = 0.569$ D^{-1} one can fairly well reproduce the expected quantitative relationship between the experimentally found M_{em} and $(\Delta E_{33} + \lambda_0) / h c \nu_{\text{em}}^{\text{max}}$ quantities (*cf.* Figure 9). Fairly well agreement between the computed and experimental M_{em} values can be seen that allow to conclude that the values of both k_r and k_{nr} rate constants, characterizing the radiative and non-radiative $^3\text{MLCT} \leftarrow \text{S}_0$ can be predicted with similar accuracy (*cf.* Figure 10).

An approach, similar to that presented above, allows us also discussion the transition dipole moments M_{em} values for these *fac*- $\text{Re}(\text{CO})_3^+$ complexes that exhibit emission with dominant $^3\text{LC} \rightarrow \text{S}_0$ character. In such complexes the energy gap between the emissive ^3LC state and higher energetically situated $^1\text{MLCT}$ state can be approximated through the difference between $^3\text{LC} \rightarrow \text{S}_0$ emission and $^1\text{MLCT} \leftarrow \text{S}_0$ absorption maxima. For the studied $[\text{Re}(\text{CO})_3(\text{N}\text{N})(\text{CH}_3\text{CN})]^+$ complexes with $\text{N}\text{N} = 47\text{dmphen}$ or tmphen ligands the estimated values of ΔE_{ST} (0.46–0.68 eV) are *ca.* 1.5–2 times smaller than the difference $h c \nu_{\text{abs}}^{\text{max}} - h c \nu_{\text{em}}^{\text{max}}$ characterizing their $[\text{Re}(\text{CO})_3(\text{N}\text{N})(t\text{-BuNC})]^+$ analogues. Thus for the complexes with the axial ligand *t*-BuNC one can expect adequately smaller M_{em} values characterizing their room temperature $^3\text{LC} \rightarrow \text{S}_0$ emission. According to the literature ϕ_{em} and τ_{em} data⁴² the M_{em} values are as small as 0.032 and 0.024 D can be estimated for $[\text{Re}(\text{CO})_3(47\text{dmphen})(t\text{-BuNC})]^+$ or $[\text{Re}(\text{CO})_3(\text{tmphen})(t\text{-BuNC})]^+$, respectively. The corresponding M_{em} values, 0.045 and 0.049 D found respectively for $[\text{Re}(\text{CO})_3(\text{tmphen})(\text{CH}_3\text{CN})]^+$ and $[\text{Re}(\text{CO})_3(47\text{dmphen})(\text{CH}_3\text{CN})]^+$ complexes are *ca.* 1.5 and

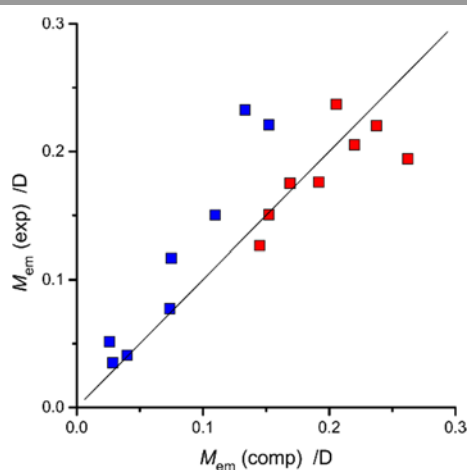


Fig. 9 Relationship between the computed and experimental values of the transition dipole moments M_{em} of $^3\text{MLCT} \rightarrow \text{S}_0$ transitions for the investigated. $[\text{Re}(\text{CO})_3(\text{N}\text{N})\text{Cl}]$ (red symbols) and $[\text{Re}(\text{CO})_3(\text{N}\text{N})(\text{CH}_3\text{CN})]^+$ (blue symbols) complexes. The solid line represents linear fit with the intercept value equal zero.

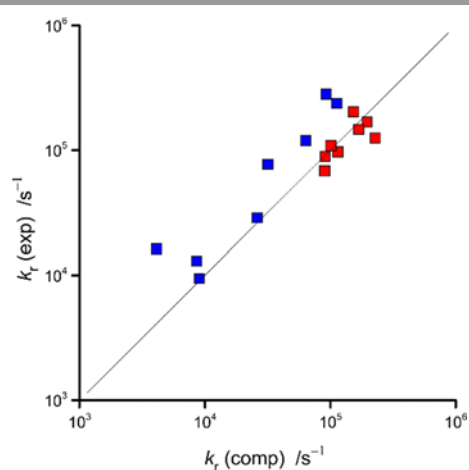


Fig. 10 Relationship between the computed and experimental values of the radiative k_r rate constants of $^3\text{MLCT} \rightarrow \text{S}_0$ transitions for the investigated. $[\text{Re}(\text{CO})_3(\text{N}\text{N})\text{Cl}]$ (red symbols) and $[\text{Re}(\text{CO})_3(\text{N}\text{N})(\text{CH}_3\text{CN})]^+$ (blue symbols) complexes.

Table 3. Summary of the FT-IR (CH₂Cl₂ solutions) and ¹H NMR (CDCl₃ solutions) data for the investigated cationic [Re(CO)₃(N∩N)(CH₃CN)]⁺ and neutral [Re(CO)₃(N∩N)Cl] complexes.

Complex type	FT-IR*	¹ H NMR
Ligand N∩N	$\nu_{\text{C-O}} / \text{cm}^{-1}$	$\delta / \text{ppm vs. TMS}$
[Re(CO)₃(N∩N)(CH₃CN)]⁺		
dpphen	2039, 1938	9.33 (2 H, d), 8.14 (2 H, s), 7.89 (2 H, d), 7.55-7.65 (10 H, m), 2.17 (3H, s)
bpy	2038, 1936	8.93 (2 H, d), 8.56 (2 H, d), 8.23 (2 H, t), 7.64 (2 H, t), 2.22 (3 H, s)
dbbpy	2038, 1935	8.77 (2 H, d), 8.37 (2 H, d), 7.58 (2 H, dd), 2.19 (3 H, s), 1.46 (18 H, s)
phen	2041, 1938	9.34 (2 H, dd), 8.75 (2 H, dd), 8.15 (2 H, s), 8.01 (2 H, dd), 2.11 (3 H, s)
29dmphen	2041, 1938	8.51 (2 H, d), 7.99 (2 H, s), 7.88 (2 H, d), 3.31 (6 H, s), 2.11 (3 H, s)
56dmphen	2041, 1938	9.25 (2 H, dd), 8.88 (2 H, dd), 7.98 (2 H, dd), 2.86 (6 H, s), 2.07 (3 H, s)
47dmphen	2039, 1936	9.13 (2 H, d), 8.27 (2 H, s), 7.77 (2 H, d), 3.00 (3 H, s), 2.09 (3 H, s)
tmphen	2038, 1935	8.99 (2 H, s), 8.24 (2 H, s), 2.86 (6 H, s), 2.67 (6 H, s), 2.07 (3 H, s)
[Re(CO)₃(N∩N)Cl]		
dpphen	2021, 1919, 1896	9.44 (2 H, d), 8.05 (2 H, s), 7.80 (2 H, d), 7.55-7.65 (10 H, m)
bpy	2123, 1919, 1898	9.09 (2 H, d), 8.21 (2 H, d), 8.09 (2 H, t), 7.56 (2 H, t)
dbbpy	2021, 1917, 1894	8.88 (2 H, d), 8.75 (2 H, d), 7.74 (2 H, dd), 1.44 (18 H, s)
phen	2023, 1921, 1898	9.42 (2 H, dd), 8.57 (2 H, dd), 8.04 (2 H, s), 7.90 (2 H, dd)
29dmphen	2021, 1915, 1896	8.34 (2 H, d), 7.86 (2 H, s), 7.75 (2 H, d), 3.35 (6 H, s)
56dmphen	2021, 1917, 1897	9.35 (2 H, dd), 8.71 (2 H, dd), 7.88 (2 H, dd), 2.81 (6 H, s)
47dmphen	2021, 1917, 1894	9.24 (2 H, d), 8.18 (2 H, s), 7.67 (2 H, d), 2.93 (6 H, s)
tmphen	2023, 1919, 1896	9.12 (2 H, s), 8.15 (2 H, s), 2.79 (6 H, s), 2.63 (6 H, s)

* The neutral [Re(CO)₃(N∩N)Cl] chelates display three bands in the CO stretching vibration region, whereas for the cationic [Re(CO)₃(N∩N)(CH₃CN)]⁺ complexes only two CO stretching vibration bands are observed because the A' (2) and A'' modes are superimposed into a single broad band.^{35,39}

1.9 times larger than those characterizing their *t*-BuCN counterparts. The observed agreement additionally supports validity of the approach applied in this work, demonstrating that the same set of main parameters can be applied in the quantitative interpretation of ³*LC/³*MLCT systems, including those with the nearly "pure" ³*MLCT character as well as those with the prevailing ³*LC contributions.

Conclusions

Similarly to our previously published work³² describing the heteroleptic [OsCl(CO)(P∩P)(N∩N)]⁺ chelates with α -diimine N∩N and bidentate phosphine P∩P ligands, the results presented in this paper illustrate a close connection between the radiative and non-radiative deactivation of the excited states with the MLCT character. In the reported studies the luminescence properties of the heteroleptic [Re(CO)₃(N∩N)Cl] and [Re(CO)₃(N∩N)(CH₃CN)]⁺ chelates have been primarily analysed within the framework of the combined Mulliken-Hush and Marcus-Jortner formalism. Regardless of all approximations applied in the performed analyses one can conclude the evidence for the theoretically expected relation between rates of the radiative and non-radiative deactivation of the excited ³*[Re(CO)₃(N∩N)Cl] and ³*[Re(CO)₃(N∩N)(CH₃CN)]⁺ states. By analysing ordinary spectroscopic data one can obtain the thermodynamic quantities relevant to molecular changes associated with MLCT phenomena as well as characterize the electronic and spin-orbit interaction affecting dominantly the properties of the luminescent ³*MLCT state. The presented results point to applicability of this approach in description of the nearly "pure" ³*MLCT systems as well as the systems

possessing the mixed ³*MLCT/³*LC character. One can also anticipate that the luminescence properties of other transition metal complexes exhibiting the MLCT emission can be analysed in a similar manner but further studies are necessary to finally confirm this possibility.

EXPERIMENTAL

Materials

Commercially available N∩N ligands (purchased from Lancaster, Alfa Aesar or Aldrich companies) and Re(CO)₅Cl (Strem Chemicals) were used in preparation of the investigated [Re(CO)₃(N∩N)Cl] and [Re(CO)₃(N∩N)(CH₃CN)]⁺ complexes. Procedures already described in the literature have been applied in the performed syntheses.^{35-39,69,73,75-77} All of the neutral [Re(CO)₃(N∩N)Cl] chelates were prepared by reacting equimolar mixtures of Re(CO)₅Cl and appropriate N∩N ligand in refluxing toluene under argon for 4-5 h. The precipitated solids were filtered after cooling of the reaction mixtures to room temperature. The investigated cationic [Re(CO)₃(N∩N)(CH₃CN)]⁺ complexes were synthesized (in the form of PF₆⁻ salts) by metathesis of their neutral congeners. The substrates were dehalogenized by reacting with equimolar amounts of AgClO₄ in refluxing acetonitrile solutions under argon atmosphere in dark for 8 h. In each case, the precipitated AgCl was filtered off before adding KPF₆ in ca. 10-fold excess. The precipitated ionic [Re(CO)₃(N∩N)(CH₃CN)]⁺...PF₆⁻ products were further filtered and dried under vacuum. The obtained complexes were purified by means of column chromatography and their structures were

confirmed using ^1H NMR and FT-IR spectroscopy (data collected in Table 3).

Instrumentation and procedures

FT-IR and ^1H NMR spectra were acquired with a Shimadzu IRAffinity-1 and a VARIAN 400-MR spectrometers, respectively. UV-vis absorption spectra were measured with a Shimadzu UV 3100 spectrometer, whereas corrected steady-state luminescence spectra and emission decays by means of a Gilden Photonics FluoroSense and FluoroSense-P fluorimeters. Room temperature absorption and emission measurements were performed in the spectroscopic grade acetonitrile solutions. In the case of emission studies the investigated solutions were carefully deaerated by the prolonged saturation with preliminary purified and dried argon. As a quantum yield standard a solution of quinine sulfate in 0.1 N H_2SO_4 ($\phi_{\text{em}} = 0.51$) was used.

Emission spectra were fitted by means of a least-square method using OriginPro 9.0 software (Origin Lab Corp.) with user-defined functions. The experimental decay curves were analysed by the single-curve method using the reference convolution based on the Marquardt algorithm with the χ^2 test and the distribution of residuals served as the main criteria in the evaluation of fit quality.

Notes and references

- A. Hagfeldt and M. Grätzel, *Acc. Chem. Res.*, 2000, **33**, 269-277.
- A. S. Polo, M. K. Itokazu and N.Y. Murakami Iha, *Coord. Chem. Rev.*, 2004, **248**, 1343-1361.
- G. C. Vougioukalakis, A. I. Philippopoulos, T. Stergiopoulos and P. Falaras, *Coord. Chem. Rev.*, 2011, **255**, 2602-2621.
- H. Yersin, A. F. Rausch, R. Czerwiec, T. Hofbeck and T. Fischer, *Coord. Chem. Rev.*, 2011, **255**, 2622-2652.
- L. Xiao, Z. Chen, B. Qu, J. Luo, S. Kong, Q. Gong and J. Kido, *Adv. Mater.*, 2011, **23**, 926-952.
- R. D. Costa, E. Ortí, H. J. Bolink, F. Monti, G. Accorsi, and N. Armaroli, *Angew. Chem. Int. Ed.*, 2012, **51**, 8178-8211.
- V. Fernandez-Moreira, F.L. Thorp-Greenwood and M.P. Coogan, *Chem. Commun.* 2010, **46**, 186-202.
- Q. Zhao, F. Li and C. Huang, *Chem. Soc. Rev.*, 2010, **39**, 3007-3030.
- K. K.-W. Lo, A. W.-T. Choi and W. H.-T. Law, *Dalton Trans.*, 2012, **41**, 6021-6047.
- K. Zeitler, *Angew. Chem., Int. Ed.*, 2009, **48**, 9785-9789.
- M. Wang, K. Han, S. Zhang and L. Sun, *Coord. Chem. Rev.*, 2015, **287**, 1-14.
- G. F. Manbeck and K. J. Brewer, *Coord. Chem. Rev.*, 2013, **257**, 1660-1675.
- A. R. Chakravarty and M. Roy, *Prog. Inorg. Chem.*, 2011, **57**, 119-202.
- H. Ali and J. E. van Lier, *Chem. Rev.*, 1999, **29**, 2379-2450.
- E. Ruggiero, S. Alonso-de Castro, A. Habtemariam and L. Salassa, *Struct. Bond.*, 2015, **165**, 69-108.
- V. Balzani and S. Campagna (Eds.), Photochemistry and Photophysics of Coordination Compounds I, *Top. Curr. Chem.*, 2007, **280**, (whole issue).
- V. Balzani and S. Campagna (Eds.), Photochemistry and Photophysics of Coordination Compounds II, *Top. Curr. Chem.*, 2007, **281**, (whole issue).
- D. J. Stufkens and A. Vlček Jr., *Coord. Chem. Rev.*, 1998, **177**, 127-179.
- A. Vogler and H. Kunkely, *Coord. Chem. Rev.*, 2000, **200-202**, 991-1008.
- D. R. Striplin and G. A. Crosby, *Coord. Chem. Rev.*, 2001, **211**, 163-175.
- A. Coleman, C. Brennan, J. G. Vos and M. T. Pryce, *Coord. Chem. Rev.*, 2008, **252**, 2585-2595.
- A. Kumar, S.-S. Sun and A. J. Lees, *Top. Organomet. Chem.*, 2010, **29**, 1-35.
- V. W.-W. Yam and K. M.-C. Wong, *Chem. Commun.*, 2011, **47**, 11579-11592.
- D. W. Thompson, A. Ito and T. J. Meyer, *Pure Appl. Chem.*, 2013, **85**, 1257-1305.
- X.-Y. Wang, A. Del Guerso and R. H. Schmehl, *J. Photochem. Photobiol. C*, 2004, **5**, 55-77.
- Z. R. Grabowski, K. Rotkiewicz and W. Rettig, *Chem. Rev.*, 2003, **103**, 3899-4031.
- N. Mataga, H. Chosrowjan and S. Taniguchi, *J. Photochem. Photobiol. C*, 2005, **6**, 37-79.
- M. D. Newton, *Coord. Chem. Rev.*, 2003, **238-239**, 167-185.
- X.-Y. Wang, A. Del Guerso and R. H. Schmehl, *J. Photochem. Photobiol. C*, 2004, **5**, 55-77.
- J. F. Endicott, Y.-J. Chen and P. Xie, *Coord. Chem. Rev.*, 2005, **249**, 343-373.
- A. Ito and T. J. Meyer, *Phys. Chem. Chem. Phys.*, 2012, **14**, 13731-13745.
- A. Kamecka and A. Kapturkiewicz, *Phys. Chem. Chem. Phys.*, 2005, **17**, 23332-23345.
- C. J. Cramer and D. G. Truhlar, *Phys. Chem. Chem. Phys.*, 2009, **11**, 10757-10816.
- T. A. Niehaus, T. Hofbeck and H. Yersin, *RSC Adv.*, 2015, **5**, 63318-63329.
- J. V. Caspar and T. J. Meyer, *J. Phys. Chem.* 1983, **87**, 952-957.
- L. A. Worl, R. Duesing, P. Chen, L. Della Ciana and T. J. Meyer, *J. Chem. Soc. Dalton Trans.*, 1991, 849-858.
- P. Y. Chen, R. Duesing, D. K. Graff and T. J. Meyer, *J. Phys. Chem.*, 1991, **95**, 5850-5858.
- M. Wrighton and D. L. Morse, *J. Am. Chem. Soc.*, 1974, **96**, 998-1003.
- S. M. Fredericks, J. C. Luong and M. S. Wrighton, *J. Am. Chem. Soc.*, 1979, **101**, 7415-7417.
- L. Wallace and D. P. Rillema, *Inorg. Chem.*, 1993, **32**, 3836-3843.
- J. M. Villegas, S. R. Stoyanov, W. Huang and D. P. Rillema, *Inorg. Chem.*, 2005, **44**, 2297-
- L. Sacksteder, M. Lee, J. N. Demas and B. A. DeGraff *J. Am. Chem. Soc.*, 1993, **115**, 8230-8238.
- R. S. Mulliken and W. B. Person, *Molecular Complexes*. Wiley, New York, 1969.
- J. B. Birks, *Photophysics of Aromatic Molecules*, Wiley, New York, 1978.
- J. Michl, E. W. Thulstrup, *Spectroscopy with Polarized Light*, VCH, New York, 1986.
- N. S. Hush, *Prog. Inorg. Chem.*, 1967, **8**, 391-444.
- N. S. Hush, *Electrochim. Acta*, 1968, **13**, 1005-1023.
- J. Ulstrup and J. Jortner, *J. Chem. Phys.* 1975, **63**, 4358-4368.
- R. A. Marcus and N. Sutin, *Biochim. Biophys. Acta*, 1985, **811**, 265-322.
- B. S. Brunschwig, S. Ehrenson and N. Sutin, *J. Phys. Chem.*, 1987, **91**, 4714-4723.
- R. A. Marcus, *J. Phys. Chem.*, 1989, **93**, 3078-3086.
- J. T. Hupp, G. A. Neyhart, T. J. Meyer and E. M. Kober, *J. Phys. Chem.*, 1992, **96**, 10820-10830.
- S. Efrima and M. Bixon, *Chem. Phys. Lett.*, 1974, **25**, 34-37.
- S. Efrima and M. Bixon, *Chem. Phys.*, 1976, **13**, 447-460.
- J. Jortner, *J. Chem. Phys.*, 1976, **64**, 4860-4867.
- M. Bixon and J. Jortner, *J. Phys. Chem.* 1991, **95**, 1941-1944.

- 57 R. S. Mulliken, *J. Am. Chem. Soc.* 1952, **74**, 811-824.
- 58 R. S. Mulliken and W. B. Person, *Molecular Complexes: A Lecture and Reprint Volume*, Wiley, New York, 1969.
- 59 S. Haneder, E. D. Como, J. Feldmann, J. M. Lupton, C. Lennartz, P. Erk, E. Fuchs, O. Molt, I. Münster, C. Schildknecht and G. Wagenblast, *Adv. Mater.*, 2008, **20**, 3325-3330.
- 60 N. Turro, *Modern Molecular Photochemistry*. University Science Books, Palo Alto, CA, 1991.
- 61 J. N. Murrell, *J. Am. Chem. Soc.* 1959, **81**, 5037-5043.
- 62 M. Bixon, J. Jortner and J. W. Verhoeven, *J. Am. Chem. Soc.* 1994, **116**, 7349-7355.
- 63 R. S. Mulliken and W. B. Person, *Molecular Complexes: A Lecture and Reprint Volume*; Wiley, New York, 1969.
- 64 J. Cortes, H. Heitele and J. Jortner, *J. Phys. Chem.*, 1994, **98**, 2527-2536.
- 65 A. Kapturkiewicz, J. Herbich, J. Karpiuk and J. Nowacki, *J. Phys. Chem. A*, 1997, **101**, 2332-2344.
- 66 F. Paolucci, M. Marcaccio, C. Paradisi, S. Roffia, C. A. Bignozzi and C. Amatore, *J. Phys. Chem. B*, 1998, **102**, 4759-4769.
- 67 P. Christensen, A. Hamnett, A. V. G. Muir and J. A. Timney, *J. Chem. Soc. Dalton Trans.*, 1992, 1455-1463.
- 68 A. Klein, C. Vogler and W. Kaim, *Organometallics*, 1996, **15**, 236-244.
- 69 R. Czerwieńiec, A. Kapturkiewicz, J. Lipkowski and J. Nowacki, *Inorg. Chim. Acta*, 2005, **358**, 2701-2710.
- 70 M. Senoue, T. Iwaki, K. Seki and M. Yagi, *J. Photochem. Photobiol. A*, 1996, **101**, 257-263.
- 71 M. A. A. Rashid, B. Saad, El-S. M. Negim and M. I. Saleh, *World Appl. Sci. J.*, **2012**, **17**, 958-963.
- 72 R. R. Dogonadze, A. M. Kuznetsov and T. A. Marsagishvili, *Electrochim. Acta*, 1980, **25**, 1-28.
- 73 B. Machura, M. Wolff, M. Jaworska, P. Lodowski, E. Benoist, C. Carrayon, N. Saffon, R. Kruszynski and Z. Mazurak, *J. Organomet. Chem.* 2011, **696**, 3068-3075.
- 74 A. Cannizzo, A. M. Blanco-Rodríguez, A. El Nahhas, J. Šebera, S. Zálíš, A. Vlček, Jr. and M. Chergui, *J. Am. Chem. Soc.*, 2008, **130**, 8967-8974.
- 75 S.-S. Sun, P. Y. Zavalij and A. J. Lees, *Acta Cryst.* 2001, **E57**, m119-m121.
- 76 J. C. Luong, R. A. Faltynek and M. S. Wrighton, *J. Am. Chem. Soc.*, 1980, **102**, 7892-7900.
- 77 A. Otávio T. Patrocínio and N. Y. Murakami Iha, *Inorg. Chem.*, 2008, **47**, 10851-10857.